# Development and Testing of the AXBT Real-Time Editing System (ARES)

CASEY R. DENSMORE,[a] STEVEN R. JAYNE,[b] AND ELIZABETH R. SANABIA[c]

[a] *Joint Program in Oceanography/Applied Ocean Science and Engineering, Massachusetts Institute of Technology–Woods Hole Oceanographic Institution, Cambridge and Woods Hole, Massachusetts*
[b] *Woods Hole Oceanographic Institution, Woods Hole, Massachusetts*
[c] *U.S. Naval Academy, Annapolis, Maryland*

(Manuscript received 8 July 2020, in final form 30 September 2020)

ABSTRACT: Airborne expendable bathythermographs (AXBTs) are air-launched, single-use temperature–depth probes that telemeter temperature observations as VHF-modulated frequencies. This study describes the AXBT Real-Time Editing System (ARES), which is composed of two components: the ARES Data Acquisition System, which receives telemetered temperature–depth profiles with no external hardware other than a VHF radio receiver, and the ARES Profile Editing System, which quality controls AXBT temperature–depth profiles. The ARES Data Acquisition System performs fast Fourier transforms on windowed segments of the demodulated signal transmitted from the AXBT. For each segment, temperature is determined from peak frequency and depth from elapsed time since profile start. Valid signals are distinguished from noise by comparing peak signal levels and signal-to-noise ratios to predetermined thresholds. When evaluated using 387 profiles, the ARES Data Acquisition System produced temperature–depth profiles nearly identical to those generated using a Sippican MK-21 processor, while reducing the amount of noise from VHF interference included in those profiles. The ARES Profile Editor applies a series of automated checks to identify and correct common profile discrepancies before displaying the profile on an editing interface that provides simple user controls to make additional corrections. When evaluated against 1177 tropical Atlantic and Pacific AXBT profiles, the ARES automated quality control system successfully corrected 87% of the profiles without any required manual intervention. Necessary future work includes improvements to the automated quality control algorithm and algorithm evaluation against a broader dataset of temperature–depth profiles from around the world across all seasons.

KEYWORDS: Ocean; In situ oceanic observations; Profilers, oceanic

## 1. Introduction

Obtaining in situ temperature–depth profiles remains a necessity for observational oceanography. While significant advances in satellite capabilities have enabled global sea surface temperature observation, resolving subsurface features (e.g., mixed layer depth and ocean heat content) and observing conditions under extremely cloudy skies require in situ measurements (Legler et al. 2015). The expendable bathythermograph (XBT) is a commonly used ship-launched sensor capable of collecting a single temperature–depth profile, and the air-launched variant, the airborne expendable bathythermograph (AXBT; Sessions et al. 1975), enables aircraft to measure upper-ocean temperatures in remote or inhospitable regions that are difficult to access by ship.

After being launched from an aircraft, an AXBT descends to the ocean surface beneath a small parachute. Once on the surface, a small bag attached to the surface float inflates to provide buoyancy, the parachute detaches, and a saltwater-activated battery in the surface float begins transmitting a VHF signal from the AXBT. Simultaneously, water-soluble tape holding a temperature probe to the surface float dissolves and releases the probe to descend through the water column. As the probe descends, a thermistor measures in situ temperatures and relays them to the surface through a thin wire, encoded as temperature-dependent, audio-range frequencies by a voltage-controlled oscillator. The surface float modulates these audio-range frequencies into one of 99 standard sonobuoy VHF carrier frequencies between 136 and 173.5 MHz, and telemeters the signal to the observing aircraft. After the profile is complete, the relay wire severs, transmission stops, and the surface float self-scuttles (Bane and Sessions 1984; Boyd 1987).

As it is received, the AXBT-transmitted VHF signal must be demodulated and Fourier transformed to identify the encoded audio-range frequency. Multiple systems have been developed to receive and process data from AXBTs, such as the MK-21 Data Acquisition System (Sippican 2003) and the Ocean Data Acquisition and Analysis Recorder (ODAAR; Grempler 1993). As the received frequencies are continuously converted to temperature measurements, the corresponding depths are obtained using an estimated probe fall rate through the water column. These conversions are the source of a host of literature aiming to identify uncertainty and correct for several error sources such as internal noise and thermal lag (e.g., Heinmiller et al. 1983; Bane and Sessions 1984; Boyd 1987; Roemmich and Cornuelle 1987; Boyd and Linzell 1993; Alappattu and Wang 2015; for a discussion, see Cheng et al. 2016). After the AXBT has finished transmitting, the received profile generally must be quality controlled to correct for noise, interference, and AXBT measurement errors using a program such as the System for At-Sea Environmental Analysis (SASEA; Hanson 1989). Fully automated processing systems are known to exist, but are not

*Corresponding author*: Casey R. Densmore, densmore@alum.mit.edu

DOI: 10.1175/JTECH-D-20-0110.1

documented in published literature (S. Paul, NOAA Aircraft Operations Center, 2020, personal communication).

Applications for AXBTs range from scientific (e.g., observations of upper-ocean processes, particularly in remote or inhospitable conditions) to military (e.g., underwater acoustics). One recent example of scientific use of AXBTs, which served as the motivation for this paper, is the Training and Research in Oceanic and atmospheric Processes In tropical Cyclones (TROPIC) field campaign (Sanabia et al. 2013). In TROPIC, upper ocean temperature observations are collected beneath tropical cyclones, transmitted globally, and assimilated into coupled numerical models to improve hurricane forecasts. From 2011 to 2019, the TROPIC team used a Mobile Ocean Observing System (MOOS) designed and built by the Naval Research Laboratory (NRL) with an integrated MK-10 Receiver and MK-21 Data Acquisition System to process AXBT data on board U.S. Air Force 53rd Weather Reconnaissance Squadron WC-130J aircraft. Temperature–depth profiles were manually quality controlled using the System for At-Sea Environmental Analysis (SASEA), a software package operated in a MATLAB environment.

ARES was developed in coordination with TROPIC as a data acquisition and quality control solution to replace the existing MOOS-SASEA system and accomplish five objectives:

1) Incorporate most hardware-defined features from MOOS as software-defined functions (to reduce the amount of necessary hardware)
2) Enable simultaneous processing of multiple AXBTs on different VHF channels
3) Integrate system date and time inputs and a connected GPS receiver to autopopulate fields on AXBT launch (and minimize errors due to incorrectly entered drop information)
4) Combine data acquisition and profile editing into a program with a single graphical user interface so users can seamlessly transition from data receipt to quality control
5) Minimize requisite oceanographic background knowledge on the part of users receiving and quality controlling AXBT-measured profiles

ARES is composed of two integrated subsystems: data acquisition (which demodulates and Fourier transforms received VHF signals before calculating the encoded temperature–depth profile) and profile editing (which applies automatic quality control checks to correct for common issues and presents the resulting profile to the user to make any additional corrections before saving). These two components are described in detail in section 2, and their performance is evaluated against the 2011–19 TROPIC dataset in section 3. Finally, ARES functionality is summarized and future work is outlined in section 4.

## 2. ARES overview

The AXBT Real-Time Editing System (ARES) was developed in Python using the PyQt5 binding for the Qt toolkit to provide a user interface, and consists of two independent subsystems. The ARES Data Acquisition System fast Fourier transforms pulse code modulated (PCM) audio signals into a raw AXBT temperature–depth profile, and displays received data in both graphical and tabular formats alongside a simple interface for users to control connected VHF receivers and input profile metadata (Fig. 1, top). The ARES Profile Editing System applies automatic checks to the raw temperature–depth profile before providing a simple interface through which users can make any additional necessary corrections (Fig. 1, bottom) and export the profile in a variety of file formats. These components are discussed separately in the following sections.

### *a. ARES Data Acquisition System*

In the current configuration, a WiNRADIO receiver connected to the aircraft's VHF antenna demodulates the received VHF signal and transfers the demodulated PCM digital audio data to the processing computer. All signal processing and subsequent computations are conducted on segments of PCM data accessed by the Data Acquisition System. Hardware integration and software-defined computations are discussed separately below.

#### 1) RADIO RECEIVER INTEGRATION AND DATA FLOW

The software-defined radio receiver currently integrated with ARES is a WiNRADIO WR-G39WSBe Sonobuoy Receiver (www.winradio.com/home/g39wsbe.htm). It demodulates transmitted FM signals from standard sonobuoy VHF carrier frequencies between 136 and 173.5 MHz, and outputs analog (SMA) and digital (serial) demodulated data.

Because a single receiver can only demodulate one VHF frequency and thus only process data from one AXBT at a time, the temporal (and given the aircraft's ground speed, spatial) constraint on which AXBTs can be launched depends on the time each AXBT takes to profile and the number of receivers in use. ARES was configured for the operation of up to six receivers in parallel using multithreading support provided in PyQt5. This number is easily adjustable in the source code, but computational power gives a secondary constraint of approximately 5–10 concurrent AXBTs (depending on the processing platform's clock rate and available random access memory).

The hardware system (composed of RF receivers, a power strip, and a USB hub) accompanying ARES requires three connections: a standard 60Hz–110V input power supply, a Bayonet Neill–Concelman (BNC) coaxial connection to a VHF antenna for RF signal input, and USB output connected to the processing computer running ARES. The VHF signals received by the connected antenna are demodulated by the WiNRADIO receiver, which outputs a stream of PCM data collected at 64 kHz from a serial port. This data stream is transferred to the processing computer using a serial to USB converter and appended to a buffer on the computer using the receiver's application-programming interface. This buffer is periodically (at approximately 10 Hz) accessed by the ARES signal processing interface to generate a temperature–depth profile from the received data stream (Fig. 2).

In addition to the required proprietary system drivers (which currently exist for Windows only), a dynamic-link library provides the application-programming interface (API)

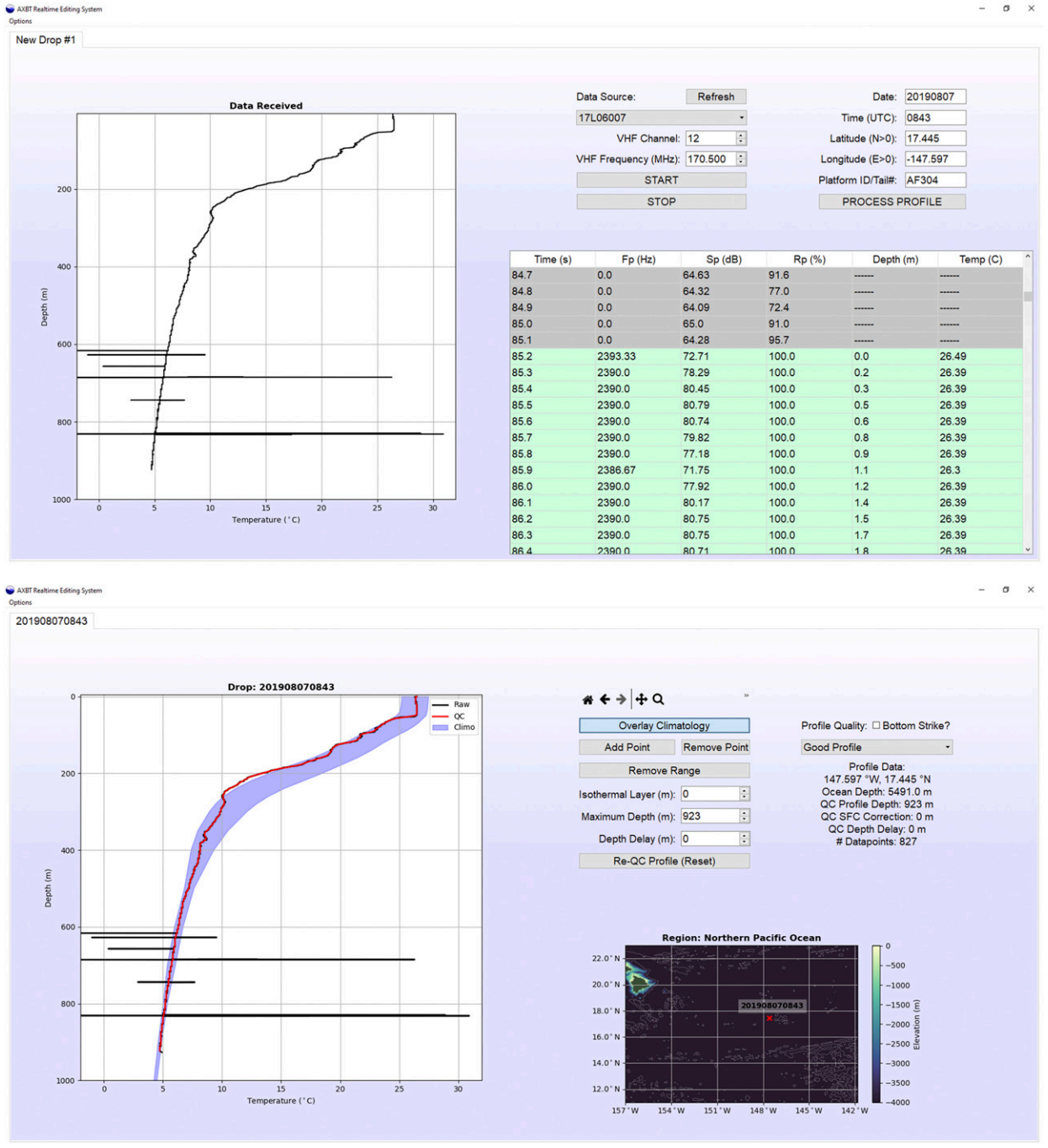


FIG. 1. Screenshots of (top) the AXBT Real-Time Editing System (ARES) Data Acquisition System and (bottom) Profile Editor interfaces.

necessary for the processing computer to communicate with and control the WiNRADIO receivers. This API includes a large range of functions for receiver communication and control (an exhaustive list is available at www.winradio.com/home/g39wsb_sdk.htm), and was used in conjunction with the Python ctypes module (Kloss 2009) to handle all receiver communication and control entirely in Python. While the exact API functions used by the Data Acquisition System would vary when integrated with a different software-defined receiver, the format would be similar and all operations after demodulated PCM data are accessed by the processing computer would be identical.

A WiNRADIO API function is used to control PCM data transfer from the receiver to the processing computer. This

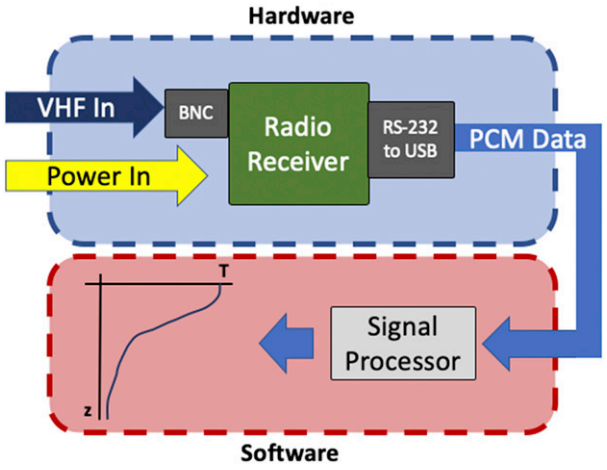


FIG. 2. Process to demodulate received a AXBT VHF signal and generate the encoded temperature–depth profile.

assigns a callback function that is executed every time a 2 KB buffer on the receiver is filled (16-bit PCM data are collected at 64 kHz in a 2 KB buffer on the receiver, so this occurs at approximately 30 Hz). The buffer contains 1 s of PCM data (64 000 points) and is length conserving, so as new values are appended to the tail of the buffer an equal number are removed from the head. In ARES, this callback function appends the data to both a WAV file and a buffer on the computer from which PCM segments are pulled by the Data Acquisition System and analyzed, as outlined in Fig. 3.

### 2) SIGNAL PROCESSING

Whether PCM data are read from a WAV file or accessed real time from a connected VHF receiver, the subsequent signal processing sequence is identical. First peak frequency, signal level, and signal-to-noise ratio are determined using a discrete Fourier transform of each segment of tapered PCM data, and then these values are used to infer the temperature–depth profile observed by the AXBT (Fig. 3).

Peak frequency, which is empirically related to the AXBT-observed ocean temperature, is determined by applying fast Fourier transforms to small subsets of data. Unless otherwise specified, a window length of 0.3 s is used (the effects of this window length are considered in section 3a). Before a data subset is transformed into the frequency domain, a cosine (Tukey) taper is applied to the time series in order to minimize spectral leakage [Eq. (1)]. The taper window ($T$) is determined by the length of the PCM data subset ($L$) and a single parameter ($\alpha$). The alpha parameter is the ratio of the tapered component of the time series to the total length of the time series, and is constrained by $0 \leq \alpha \leq 1$:

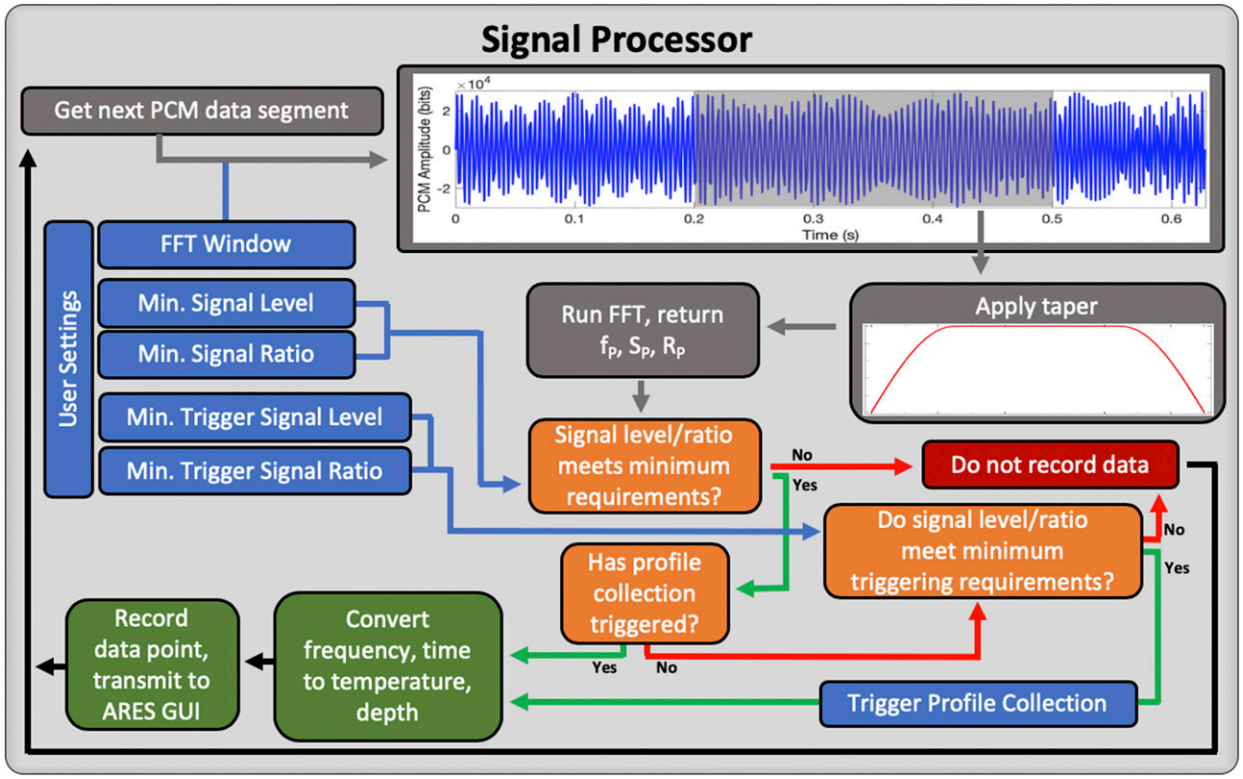


FIG. 3. Sequence to pull and process segments of PCM data to identify valid temperature–depth measurements transmitted from an AXBT.

$$T[i]=\begin{cases}\frac{1}{2}\left[1+\cos\left(\frac{2\pi}{\alpha}\frac{i-1}{L-1}-\pi\right)\right], & i<\frac{\alpha}{2}(L-1)+1\\ \frac{1}{2}\left[1+\cos\left(\frac{2\pi}{\alpha}-\frac{2\pi}{\alpha}\frac{i-1}{L-1}-\pi\right)\right], & i>L-\frac{\alpha}{2}(L-1)\\ 1, & \text{otherwise}\end{cases}. \tag{1}$$

The frequency spectra for a given segment of PCM data are calculated using a fast Fourier transform (requiring only the PCM data subset and corresponding sampling frequency), using the numpy.fft.fft( ) function included in Python's NumPy module (Oliphant 2006). The transform of a discrete time series ($s$, of length $L$ and sampling frequency $f_s$) into the frequency domain ($S$) is described in Eq. (2), where $m$ and $n$ are discrete indices corresponding to elements in the time and frequency domains, respectively:

$$S[n]=\sum_{m=0}^{L-1}s_m e^{-i2\pi mn/L},$$
$$n=0,1,2,\ldots,\frac{L}{2},$$
$$\Delta f=\frac{f_s}{L},\quad f=n\Delta f. \tag{2}$$

Resulting frequency spectra ($S$) are collapsed into three characteristic parameters: the peak frequency ($f_P$) and the corresponding signal level ($S_P$) and signal-to-noise ratio [$R_P$; defined mathematically in Eq. (3)]. Only signals from 1300 to 2800 Hz, corresponding to a realistic temperature range of −3.88° to 37.7°C, are considered. The signal level depends on the maximum spectral value in the 1300–2800 Hz band (corresponding to the peak frequency that the AXBT is presumed to be transmitting), and the signal-to-noise ratio (SNR) is the ratio of that maximum spectral value in the 1300–2800 Hz band to the maximum value in the entire band. Thus, the SNR ranges between 0 and 1, where it is 0 if no nonzero values are measured in the 1300–2800 Hz band and 1 if the most powerful received signal is in the 1300–2800 Hz band. These parameters are used to distinguish AXBT signal from noise and to calculate the corresponding temperature if necessary. To be considered a valid AXBT signal, the signal level and SNR must both satisfy preset thresholds (appropriate thresholds are considered in the Data Acquisition System evaluation). Because possible maximum values of the signal spectra span several orders of magnitude, the peak signal level is expressed in decibels (dB relative to 1 bit, referred to hereafter as dB):

$$K=\arg\max S_k,\quad f[k]\in[1300,2800], \tag{3a}$$
$$f_P=f[K], \tag{3b}$$
$$S_P=10\log_{10}\left(\frac{S[K]}{1\text{ bit}}\right), \tag{3c}$$
$$R_P=\frac{S[K]}{\max S}. \tag{3d}$$

#### 3) TEMPERATURE–DEPTH CONVERSION

For signals that satisfy the minimum signal level, frequency range, and SNR requirements, temperature and depth are determined from the peak frequency and elapsed time between the current observation and first observation. ARES uses the general empirical relationship between measured temperature (°C) and transmitted frequency (Hz) [Eq. (4); Boyd 1987; note that the coefficients 1440 and 36 have units of Hz and Hz °C$^{-1}$, respectively]:

$$f=1440+36T. \tag{4}$$

Additionally, the standard probe fall rate is assumed to be 1.52 m s$^{-1}$ (Boyd 1987). Thus, given the peak frequency ($f_P$) and elapsed time ($\Delta t$) since the first observation (when it is presumed the probe is at the surface), the corresponding temperature ($T$) and depth ($z$, positive down) are calculated as

$$T=(2.778\times10^{-2})f_P-40, \tag{5a}$$
$$z=1.52\Delta t. \tag{5b}$$

Determining elapsed time requires identification of the first valid signal from the AXBT. Because AXBT signals are typically stronger when transmission begins and decay over time as distance between the float and the aircraft increases, in order to prevent VHF interference from prematurely triggering the profile, higher minimum signal level and signal-to-noise ratio thresholds are required for a signal to be accepted as the surface value. Thus, AXBT profiles are processed by repeating the six steps below at the Data Acquisition System's sampling frequency of approximately 10 Hz (this process is represented visually in Fig. 3):

1) A subset of PCM data is pulled from the input data stream and tapered.
2) The tapered PCM subset is transformed into the frequency domain.
3) Peak frequency, signal-to-noise ratio, and signal level are calculated.
4) If the signal level and SNR are above the minimum thresholds and profile collection has already been triggered, then elapsed time is calculated and the corresponding temperature and depth values are determined and recorded.
5) If profile collection has not been triggered but the signal level and SNR satisfy the trigger thresholds, then the observation time is recorded to determine future elapsed times, profile collection is triggered, and the surface temperature is calculated and recorded.
6) Profile collection is terminated by the user, typically after a period of 30 s without valid data.

### b. *ARES profile quality control*

#### 1) AUTOMATED QUALITY CONTROL ALGORITHM

The automated quality control (autoQC) algorithm corrects raw temperature–depth profiles in two steps, described separately in the following subsections. First, the profile is corrected

for common modes of VHF interference (e.g., spikes and false starts), and is smoothed and subsampled to a lower resolution (default 10 m smoothing, 1 m sampling resolution). Then the profile is compared to bathymetry and climatology data to identify (and correct when possible) bottom strikes, climatology mismatches, and other discrepancies before displaying the resulting quality-controlled profile to the user for additional edits and/or data export.

*(i) VHF interference correction*

The following VHF interference corrections are applied to raw temperature–depth profiles:

1) Gaps in data due to profile false starts are identified and corrected.
2) Spikes from interference are identified using a depth-based running standard deviation filter and removed.
3) Profiles are smoothed using a depth-based box filter.
4) Profiles are subsampled.

Gap detection identifies "false starts" due to strong, typically external signals from a source other than the observed AXBT that trigger profile collection before the AXBT begins transmitting data. These false starts are usually characterized by a brief signal at or near the surface, followed by a several-second gap in data, and then an otherwise valid AXBT profile that is depth shifted (so the actual surface temperatures from the AXBT are recorded at some subsurface depth). These are identified by searching for a break in data exceeding 10 m in the upper 50 m of the profile (as data gaps due to signal loss are less common near the surface when the AXBT signal is stronger as the aircraft is still close to the float). If such a break exists, the profile is shifted upward so the surface observation is the first data point after the gap, and the gap check is repeated until no such gaps exist in the upper 50 m.

The second step uses a running filter to identify spikes due to VHF interference. This is accomplished by calculating the mean and standard deviation for all profiles within a 10 m window of a point [$\pm 5$ m, corresponding to $D_\sigma = 5$ m in Eq. (6)]. If an individual point deviates from the mean by more than the product of a user-specified coefficient ($\beta$) and the standard deviation about the mean [such that at any index $i$, $|T[i] - \hat{T}[i]| \geq \beta\sigma_T[i]$, where $\hat{T}[i]$ and $\sigma_T[i]$ are the mean and standard deviation of the temperatures within the 10-m window of the point $z[i]$ as defined in Eq. (6)], the data point is considered a spike and discarded (for the ARES Data Acquisition System evaluation, $\beta = 1$):

$$\hat{T}[i] = \frac{1}{N}\sum_{j=1}^{N} \hat{T}_n, \quad j \in (z[i] - D_\sigma) \leq z[j] \leq (z[i] + D_\sigma),$$

$$\sigma_T[i] = \left[\frac{1}{N}\sum_{j=1}^{N}(T_j - \hat{T}[i])^2\right]^{1/2}. \tag{6}$$

After the two primary modes of VHF interference (false starts and profile spikes) are corrected if necessary, the temperature–depth profile is passed through a depth-based smoother using a simple box filter described by Eq. (7), where the depth window is determined by $D_M$, and $\overline{T}$ is the smoothed temperature profile:

$$\overline{T}[i] = \frac{1}{N}\sum_{j=1}^{N} T_j, \quad j \in (z[i] - D_M) \leq z[j] \leq (z[i] + D_M). \tag{7}$$

Finally, profiles are subsampled to a lower resolution before being displayed to the user for additional edits (as necessary) and data export. The smoothing window should be at least twice the subsampled resolution in order to prevent aliasing (noting that boxcar filters have a relatively poor frequency response compared to more advanced low-pass filters). However, the default subsampling resolution is 1 m, and in practice it was observed that a 10 m smoother ($D_M = 5$ m) was necessary to remove high-frequency variability due to remaining VHF interference.

*(ii) Comparison to bathymetry and climatology*

After being corrected for VHF interference, smoothed, and subsampled, the temperature profile is compared to bathymetry and climatology data given the AXBT launch position and date. Ocean depth at the AXBT launch position is interpolated from the NOAA ETOPO1 Global Relief Dataset (Amante and Eakins 2004), which provides global topography and bathymetry at a 1 arc-min resolution. The autoQC algorithm automatically truncates profiles at the bathymetry-indicated ocean depth.

Climatological monthly ocean temperature means and standard deviations are from subset of data from the Generalized Digital Environmental Model (GDEM) climatology (NRL 2009) that includes values at a 0.25° horizontal resolution for 29 vertical levels in the upper 1000 m. The profile climatology comparison has two steps: 1) comparing profile slopes to identify bottom strikes, and 2) comparing the observed profile to climatology to detect possible climatology mismatches (e.g., slow-falling probes, late starts, and otherwise faulty AXBTs). Because bottom strikes typically appear as temperature observations that are erroneously isothermal or warming with depth at the base of the profile, the slopes of the observed and climatological profiles are calculated and compared. To minimize incorrect identifications due to higher-frequency variability, a 50-point running mean of the differences between the climatology and observed profile slopes is examined. If this running mean exceeds 0.1°C m$^{-1}$, it is considered a bottom strike, and all data below the depth at which this threshold is exceeded are discarded. The observed profile is then compared to the climatology to identify potential profile discrepancies. If less than 50% of the observed profile falls within the uncertainty range for the climatology (currently one standard deviation), then the profile is flagged as a climatology mismatch. An example of the climatology comparisons for two adjacent AXBT profiles collected three minutes apart, one of which was a bad profile that failed to start transmitting until the probe had already reached at least 50 m, is shown in Fig. 4. Note that the good profile differs slightly from climatology, but is sufficiently within the region of climatological uncertainty to be identified as a match by the algorithm.

If either a bathymetry-based or climatology-based bottom strike is identified, the profile is truncated at that depth (priority is given to the climatology-based strike if both are identified). After a profile has been corrected for both VHF interference and bathymetry- and climatology-indicated

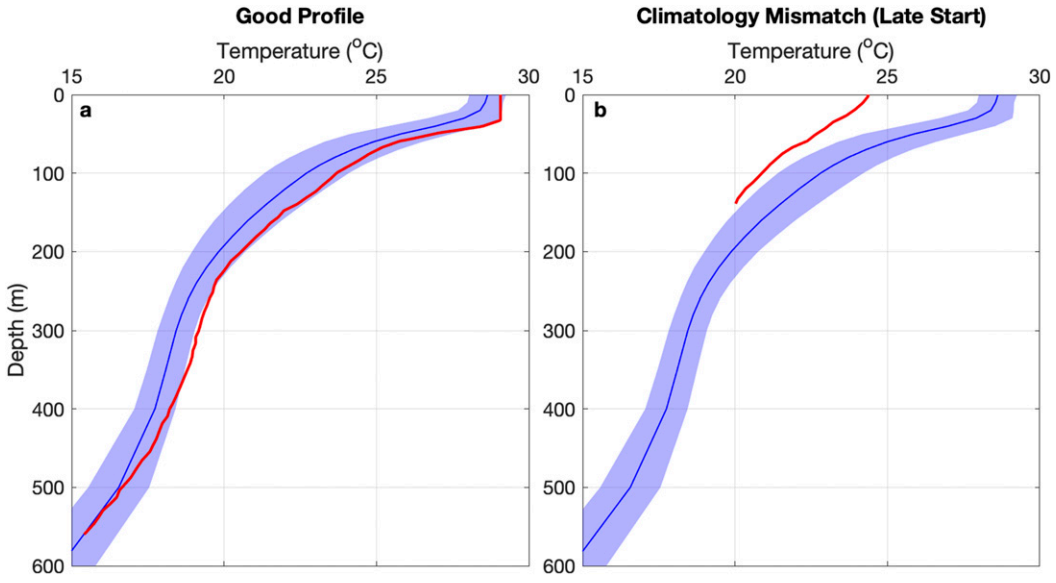


FIG. 4. Climatology comparison with adjacent (a) good and (b) bad AXBT profiles launched 3 min apart. Observed AXBT temperature profiles are shown in red and the corresponding climatological profile (given position and month) is overlaid in blue. Blue shading denotes the climatological profile plus and minus one standard deviation, which 50% or more of all observed temperature–depth points must fall within to be considered a match.

discrepancies, it is plotted on the Profile Editor interface. Original and quality-controlled profiles are overlaid in black and red (respectively) on top of blue-shaded climatology (showing plus and minus one standard deviation). When applicable, a climatology mismatch is noted with red text in the bottom-right corner of the profile window.

#### 2) USER-DEFINED QUALITY CONTROL

Users can make four categories of edits to the quality-controlled profile (listed in order of appearance on the GUI, from top to bottom):

1) Add or remove individual points or a range of points
2) Specify a surface isothermal region to remove erroneous surface spikes
3) Truncate the base of the profile to correct for bottom strikes or excessive interference
4) Vertically shift the profile to correct for VHF interference

Individually removing points or spikes may be necessary when the autoQC algorithm's spike removal feature fails to identify all erroneous data points. This is especially common when there is extreme variability due to VHF interference that saturates the standard deviation filter and increases the deviation necessary to identify a data point as erroneous. Additionally, if too many points are truncated and important profile characteristics are missed, adding individual points may be necessary. Individual points can be added and ranges of points can be added or removed with a point selection tool integrated into the ARES Profile Editor interface.

Occasionally, AXBT surface observations include erroneous spikes due to probe acclimation or interference. The ARES Profile Editor provides an option to manually create an isothermal layer at the surface by setting the temperature of all data points above a specified depth equal to the observed temperature at that depth. For example, if the surface temperature erroneously starts at 26°C at the surface, but warms to a realistic value of 28°C at 5 m, setting the isothermal layer value to 5 m will change the temperatures of all data points above 5 m to 28°C, removing the surface spike. However, care must be taken by the operator to distinguish diurnal surface heating and cooling effects from erroneous features.

In some cases, it is necessary to truncate base of the profile, either to remove data from a bottom strike or to remove excessively variable (strong-interference) data. Finally, excessive VHF interference (either noise or an unexpected signal) that falsely triggers the start of profile collection can be overlooked by the autoQC algorithm if the gap between interference and valid data is less than 5 m or the interference extends without gaps beyond 50 m. If the correct profile surface is easily identifiable, the entire profile can be shifted upward manually. User-specified surface isothermal layer generation and profile truncation are not applied until after the vertical shift, so applying a vertical shift of 200 m and profile truncation at 400 m would first shift the profile upward by 200 m, and then truncate all data that were below 600 m on the raw profile. Examples of profiles requiring each of these corrections are analyzed in section 3b.

## 3. ARES performance evaluation

### *a. Signal processing evaluation*

#### 1) METHODOLOGY

To evaluate the accuracy of the ARES signal processing package, 531 temperature–depth profiles collected with the MOOS system from 2011 to 2019 during the TROPIC field

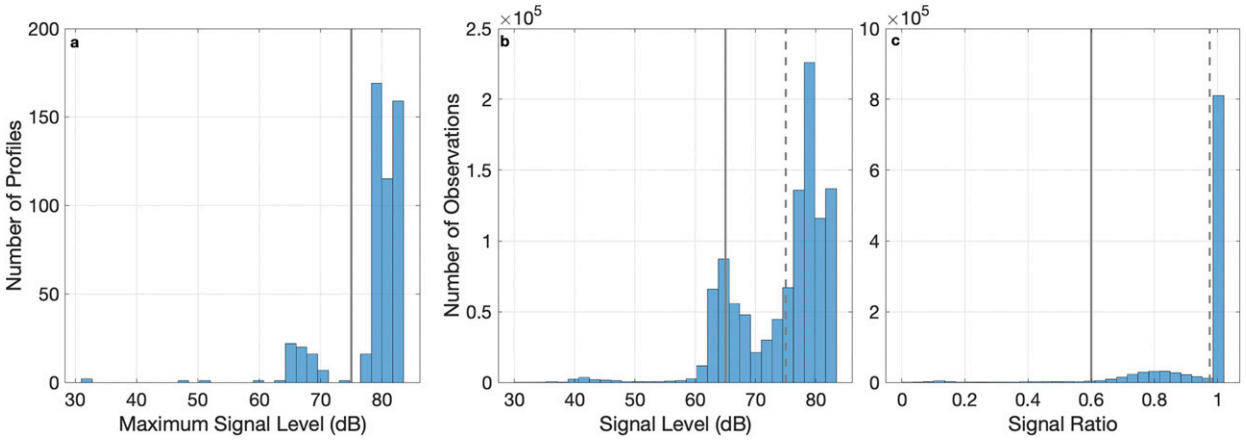


FIG. 5. (a) Distribution of maximum signal levels (dB) for the 531 reprocessed profiles. The vertical gray line denotes the required minimum peak signal level for all profiles analyzed ($S_{P_{MAX}} = 75$ dB). (b),(c) Distributions of signal levels (dB) and signal-to-noise ratios, respectively, for all observations in the 459 profiles whose maximum signal level exceeds the threshold in (a). Vertical lines represent minimum signal level and ratio thresholds (solid and dashed lines correspond to absolute minimum and trigger thresholds, respectively) applied when evaluating Data Acquisition System performance.

campaign were reprocessed from archived raw audio (.wav) files. These files contain the same format of PCM audio data as the demodulated AXBT signal that is output to the processing computer from a VHF radio receiver. Of these 531 recorded profiles, 459 profiles met minimum signal level requirements for reprocessing and 387 of those 459 profiles had corresponding ASCII files with temperature–depth profiles collected via MK-21 processor, enabling a direct comparison between ARES Data Acquisition System and MK-21 output. Given the MK-21's wide use in scientific and military applications, it can be considered an industry standard for AXBT processing. Thus, in this study the profiles processed with the MK-21 are considered to be a baseline against which the accuracy of the ARES Data Acquisition System is evaluated.

The source audio files were reprocessed at 5 Hz using windowed segments of PCM data 0.3 s in length (corresponding to 13 230 data points given a 44.1 kHz sampling frequency for all files), resulting in a 33% overlap in PCM data with each adjacent observation. Segments were tapered with a cosine taper ($\alpha = 0.5$) before being Fourier transformed into the frequency domain. The resulting profiles were then examined to optimize the minimum signal level and signal-to-noise ratio thresholds applied, determine the accuracy of collected temperature–depth profiles, and consider the effects of taper and window size on the resulting profiles.

### 2) MINIMUM THRESHOLDS FOR $S_P$ AND $R_P$

Because profiles were originally obtained with a mix of shallow- and deep-water AXBTs from multiple manufacturers and processed with multiple receivers using varying settings, the peak signal levels of the associated raw audio files also vary greatly (corresponding to peak signals spanning several orders of magnitude; Fig. 5a). To standardize the raw data analyzed, profiles with a peak signal level of less than 75 dB were excluded, leaving 459 profiles for additional analysis.

To determine optimal signal level and signal-to-noise ratio thresholds for reprocessing of the remaining 459 profiles, distributions of observed signal levels (Fig. 5b) and signal-to-noise ratios (Fig. 5c) were examined. The signal level distribution can be divided into three groupings: those greater than 70 dB, those between 60 and 70 dB, and those less than 60 dB. The first two categories are most likely dominated by valid AXBT signal whereas the third category consists primarily of noise. The bimodal nature of the first two categories highlights the remaining variability in signal levels, due to some combination of variability among AXBTs, residual differences in processing configurations, and ambient conditions (including aircraft altitude, distance from float, and atmospheric conditions).

Comparably, signal-to-noise ratios are separated into three distinct categories. The first (and by far the largest) category consists of SNR values equal to unity, which occurs when the dominant signal received by the aircraft is within the expected frequency for AXBTs (1300–2800 Hz). A second peak ranging from 0.6 to 0.9 consists of some combination of signals and noise. In this case, the greatest signal level is observed at a frequency outside of the expected range for AXBTs but a signal of approximately the same order of magnitude is observed within the AXBT frequency band. Finally, a third distribution below 0.6 most likely consists of primarily electronic noise.

In this study it is assumed that the first groupings of signal level and SNR observations consist almost exclusively of good data, the second groupings are composed of a mix of signal and noise, and the third groupings are almost exclusively noise. To optimize inclusion of good data and exclusion of noise, the minimum signal level and SNR for observations to be considered good data (Fig. 5, solid lines) were set as 65 dB and 0.6, respectively, and the minimum trigger signal level and SNR necessary to begin profile collection (Fig. 5, dashed lines) were set as 75 dB and 0.975, respectively.

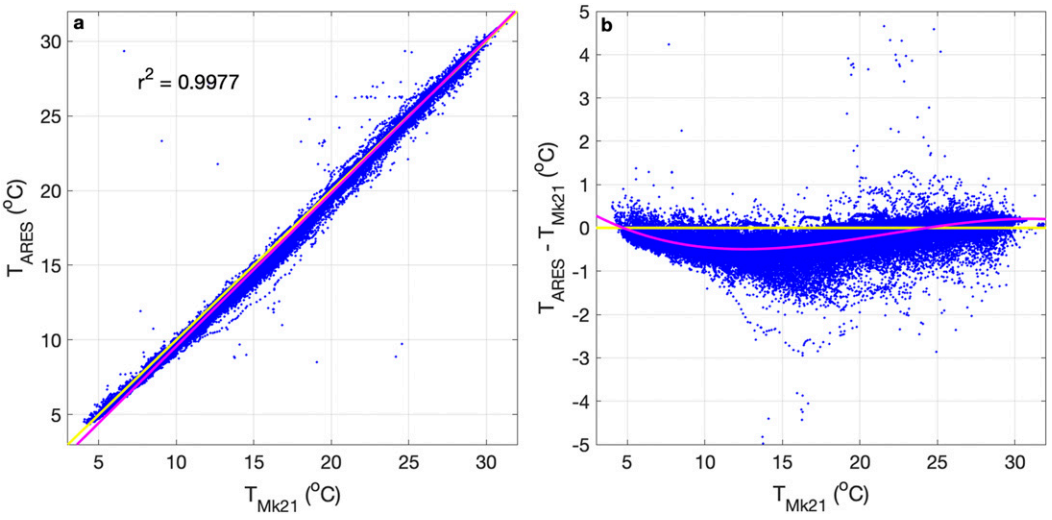


FIG. 6. Comparison of 2 m bin-averaged temperatures processed by the MK-21 and by ARES. Yellow lines denote a 1:1 relationship and magenta lines represent best fits for the data.

### 3) PROFILE ACCURACY

A comparison of MK-21- and ARES-processed temperature–depth profiles (Fig. 6) suggests that the ARES signal processing module performs comparably to the MK-21. The 2 m binned temperatures exhibit a nearly 1-to-1 relationship (note the agreement between yellow and magenta lines, and $r^2$ = 0.9977), with two exceptions. First, a small number of points more than 1°C from the 1-to-1 line along either axis are likely due to noise that was not filtered by either the ARES or MK-21 signal processing systems. Second, there is a systematic shift toward negative residuals (ARES observations are warmer than corresponding MK-21 observations) for temperatures between approximately 7° and 23°C and toward positive residuals (MK-21 observations are warmer than corresponding ARES observations) for temperatures below 7°C and above 23°C (Fig. 6b). This systematic shift is likely due to differences in the conversion equations (notably the probe fall rate equation) used in each scheme. ARES currently uses the standard Navy linear fall rate equation (Boyd 1987), whereas the MK-21 uses a higher-order, proprietary fall rate equation. It should be noted that the purpose of this analysis is to evaluate the signal processing scheme (e.g., tapering, transforming, and excluding noise) rather than to compare effectiveness of different AXBT temperature and depth conversion equations, which have been studied extensively in previous literature (e.g., Sessions et al. 1975; Bane and Sessions 1984; Boyd 1987). Substituting different conversion equations has been integrated as a user-defined setting, so users can apply custom (up to third order) temperature and depth conversions.

To quantify which processor better removed interference from temperature–depth profiles, standard deviation profiles were calculated by subdividing each profile into 10 m bins, determining the standard deviation for each bin, and comparing for MK-21- and ARES-processed profiles (Fig. 7). Because temperature changes due to noise [$O$(1–10)°C] are much greater than typical valid temperature changes on scales of 10 m or less, these binned standard deviations for a profile should quantify the interference projected onto the profile within each 10 m range. Lower standard deviations indicate that less variability due to noise was projected onto the raw temperature–depth profile by the Data Acquisition System.

ARES- and MK-21-processed profiles exhibited similar 10 m standard deviations from approximately 30 to 200 m. Both profiles have local maxima near the thermocline, where ocean temperatures can change drastically on a scale of 10 m or less. However, ARES-processed standard deviations are lower both at the surface (in the upper 30 m) and at depths greater than approximately 200 m. An increase in interference at depth is likely due to a decrease in AXBT signal strength as the receiving aircraft translates away from the float, decreasing the signal-to-noise ratio. Hence, the application of a minimum signal ratio threshold in ARES likely accounts for its better performance below 200 m.

### 4) WINDOW OPTIMIZATION AND TAPERING

Adjusting the window size ($W$) of the discrete Fourier transform results in a trade-off between computational expense and temperature resolution [$\Delta T$, Eq. (8)]. Specifically, as the window size is increased, the window length ($L$) increases and the frequency step size ($\Delta f$, in Hz) in the transformed spectra [Eq. (2)] decreases, which also decreases the corresponding temperature step size [through Eq. (4)]. This is because the sampling frequency ($f_s$), which relates window length ($L$, number of PCM data points) to both window size ($W$, in seconds) and frequency step, cancels out [Eq. (8); where the coefficient 36 has units of Hz °C$^{-1}$]:

$$\Delta T = \frac{\Delta f}{36} = \left(\frac{1}{36}\right)\left(\frac{f_s}{L}\right) = \left(\frac{1}{36}\right)\left(\frac{f_s}{f_s W}\right) = \frac{1}{36W}. \qquad (8)$$

This corresponds to a temperature resolution of 0.093°C for the standard window size of 0.3 s (Table 1). To further evaluate the resolution versus computational efficiency trade-off, 10 raw audio files were reprocessed using four different window sizes

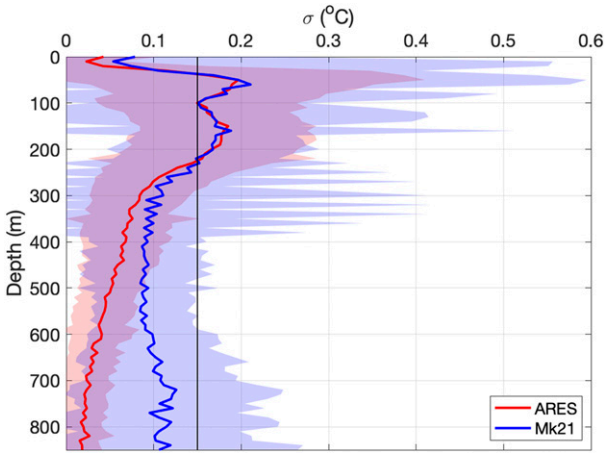


FIG. 7. Average 10 m standard deviations for temperature–depth profiles processed by the MK-21 (blue) and by ARES (red). Shading denotes plus and minus one standard deviation from the mean deviations. The black vertical line denotes 0.15°C, the rated accuracy for Sippican AXBTs (Boyd and Linzell 1993).

(0.1, 0.2, 0.3, and 0.5 s) both with and without a cosine taper. Performance effects of window size are shown in Table 1, with all performance times and standard deviations expressed as ratios to the comparable performance time using a 0.3-s window and no taper. Using window sizes of 0.1, 0.2 and 0.5 s, ARES processed files in 40%, 70%, and 285% the amount of time it took to process an identical file with a 0.3-s window (respectively). However, the corresponding temperature resolution increased from 0.28°C for a 0.1 s window to 0.006°C for a 0.5-s window. Based on these results, 0.3 s remains a suitable window size as it provides a temperature resolution better than the approximate AXBT temperature accuracy of ±0.2°C (Boyd 1987; Sippican 2003) while enabling ARES to process multiple profiles simultaneously without consuming all of the processing computer's resources.

The negligible effect of adding a cosine taper on processing time is also apparent in Table 1. The mean residual between untapered and tapered temperatures was 0.02°C, with the distribution ranging from 0.003° to 0.1°C (not shown). Additionally, mean 10 m temperature standard deviations (the same metric presented in Fig. 7) are 0.114° and 0.116°C for tapered and nontapered profiles. Despite the minimal effect of tapering on mean statistics, the potential for reduced interference on a case-by-case basis combined with the minimal associated increase in computational expense are sufficient to justify retaining Tukey taper application as a component of the signal processing data flow.

### b. *Profile quality control evaluation*

#### 1) METHODOLOGY

To examine the accuracy of the ARES Profile Editor interface, 1215 uncorrected AXBT profiles (raw data recorded with a MK-21 Processor) from the TROPIC field campaign (collected between 2011 and 2019) were reprocessed with ARES. For each observation, it was noted whether additional edits (beyond autoQC algorithm corrections) were required, if any quality control flags were applicable, and if the final profile was of satisfactory quality for transmission to the GTS for further use in numerical models (as agreed upon by four independent users). Additional profile comments and any required manual adjustments were also noted. The reprocessed profiles were evaluated against the original TROPIC dataset of profiles that were manually quality controlled with SASEA (Hanson 1989), as described in Sanabia et al. (2013).

TABLE 1. Audio file processing time means and standard deviations, and corresponding temperature resolution (°C), for several combinations of FFT windows and taper use. Processing time means and standard deviations (comma separated) are expressed as the ratio for a given processing time to the corresponding time for the same file using no taper and a window of 0.3 s.

| FFT window (s) | Resolution (°C) | No taper | With taper |
|---|---|---|---|
| 0.1 | 0.28 | 0.40, 0.06 | 0.39, 0.07 |
| 0.2 | 0.14 | 0.70, 0.10 | 0.71, 0.11 |
| 0.3 | 0.09 | 1, 0 | 1.0, 0.03 |
| 0.5 | 0.06 | 2.85, 0.19 | 2.91, 0.11 |

#### 2) PROFILE QUALITY DISTRIBUTION

Of the 1215 AXBT profiles processed, 1177 (97%) were correctable to a sufficient quality for use in numerical models (light and dark green wedges; Fig. 8a). The most common discrepancies for the remaining 38 profiles were late starts (the profile failed to start transmitting data until the probe was no longer at the surface) and isothermal profiles (typically the thermistor probe failed to physically release from the AXBT surface float, and therefore recorded only surface data rather than descending through the water column) (Fig. 8c). Of those 1177 good AXBT profiles, 156 profiles required manual user edits, leaving 1021 (87%) for which the autoQC algorithm applied sufficient profile corrections without manual intervention.

Applying the autoQC algorithm and integrating climatology and bathymetry increased operator efficiency while minimizing potential for operator error, compared to the original manual quality control method. Profiles reprocessed with ARES required less than a minute on average to quality control, with 87% of those profiles requiring no manual user intervention. This contrasts with the previous (manual) method, which typically took about 10 min to quality control per profile and required manual intervention for 100% of profiles. Additionally, the integrated bathymetry and climatology enabled operators to make more informed decisions when distinguishing profile discrepancies from actual features. Together, these resulted in a noteworthy increase in the number of profiles corrected to a quality sufficient for transmission to the GTS and assimilation in numerical models. During TROPIC, 1073 of 1215 (88%) profiles were transmitted to the GTS. Thus, the 1177 profiles (97%) successfully reprocessed with ARES yielded a 9% increase (104 profiles).

Root-mean-square differences between quality-controlled ARES- and SASEA-processed profiles remained below 0.1°C over the full range of profile depths (Fig. 9, solid line). The standard deviation of these differences exceeded 0.5°C

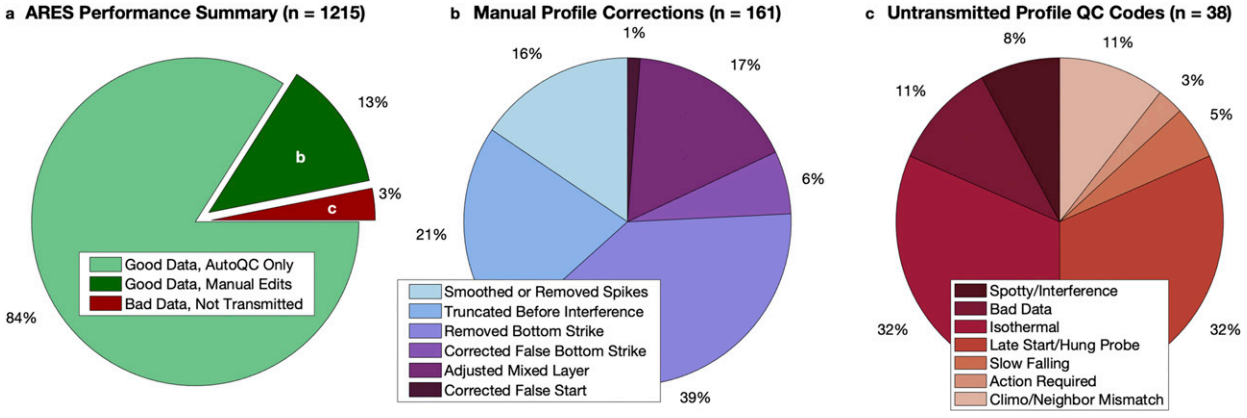


FIG. 8. Distributions of (a) autoQC algorithm performance, (b) operator corrections for profiles that required manual edits, and (c) quality control codes for bad profiles. Note that (b) and (c) show the distributions of profiles from the dark green and red wedges, respectively, in (a).

between approximately 200 and 400 m (Fig. 9, shading), corresponding to greater temperature variability in the thermocline. Additionally, there was an increase in mean profile differences and corresponding standard deviations near the surface (shallower than approximately 30 m). This suggests that either quality-controlled surface temperatures are much more sensitive to the quality control method applied, more manual corrections were applied during data reprocessing at the surface, or some combination thereof. It is worth noting that these profiles were quality controlled from the same raw data, and thus the initial data acquisition methods (including fall rate and temperature conversion equations) were the same for both sets of profiles.

### 3) COMMON AUTOQC FAILURE POINTS

In 13% of cases (Fig. 8a, dark green wedge), the autoQC algorithm was not able to sufficiently correct profile discrepancies. Features that required manual corrections fell into one of several categories (Fig. 8b):

1) Bottom strikes ($n = 73$)
2) Excessive variability at depth ($n = 34$)
3) Erroneous mixed layer features ($n = 27$)
4) Spikes due to noise and interference ($n = 25$)
5) False starts ($n = 2$)

Each of these conditions are discussed separately below, with examples in Fig. 10. Additionally, because some profiles required multiple types of corrections, the sum of all edits above ($n = 161$) is greater than the number of manually edited profiles ($n = 156$).

#### *(i) Bottom strikes*

ARES uses high resolution (1 arc-min) global bathymetry to assist in bottom strike detection. However, this check can still fail by either missing actual bottom strikes (Fig. 10a) or unnecessarily truncating good data (Fig. 10b). Bottom strike correction failures are most common in regions characterized by large bathymetric variability over small scales or when AXBTs translate a large distance from their launch point while descending through the atmosphere (e.g., in high wind conditions). Although the autoQC algorithm also uses climatology to assist in bottom strike detection by comparing profile slopes to detect erroneous warming, this check failed to identify some bottom strikes in the observed profiles. Routines could be implemented to compare profile slopes to predetermined thresholds, but this would be region specific and therefore violate the objective of developing AXBT-editing software usable in any ocean basin. Regardless, bottom strike under or overcorrection can be easily identified during manual quality control, and increasing the robustness of the climatology-assisted component of the autoQC algorithm remains a priority for future work.

#### *(ii) Excessive variability at depth*

Occasionally, some AXBT profiles become excessively spiky at depth so the autoQC algorithm's despiking and

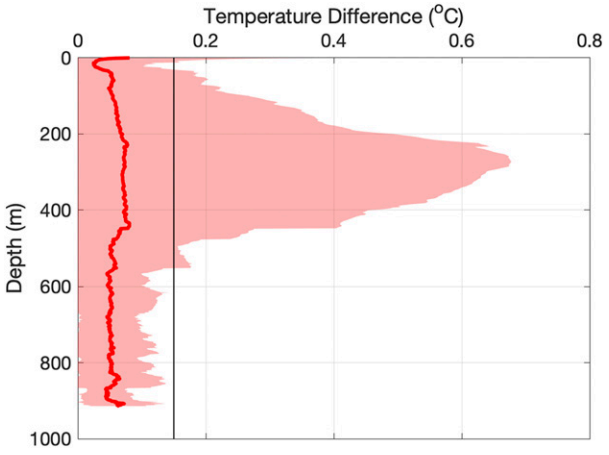


FIG. 9. Root-mean-square temperature differences (°C, solid red line) for ARES- and SASEA-processed profiles. Shading denotes mean temperature differences plus and minus one standard deviation.

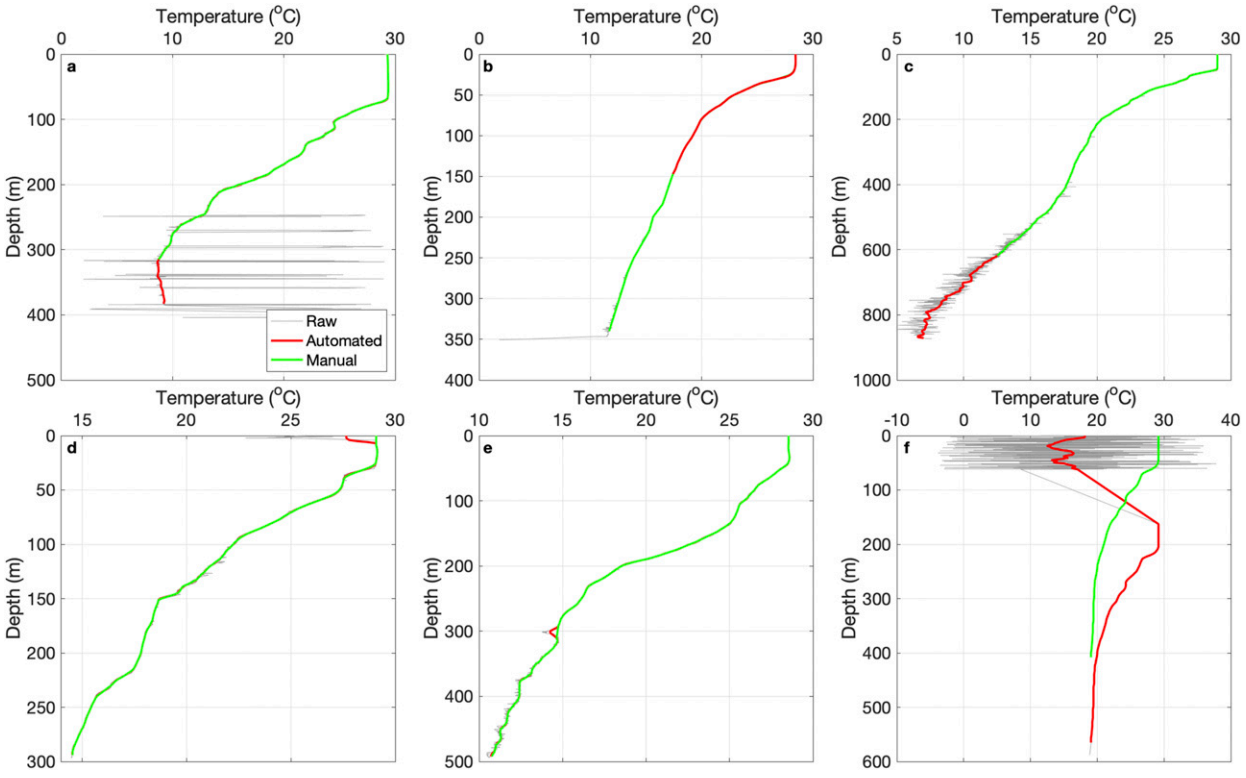


FIG. 10. Examples of profiles that required manual edits, for (a) missed bottom strike, (b) false positive bottom strike, (c) excessive interference at depth, (d) erroneous mixed layer feature, (e) temperature spike, and (f) missed profile false start. Unedited (raw) profiles are plotted as gray lines, and incorrectly (autoQC) and correctly (manually) quality-controlled profiles are overlaid in red and green, respectively.

smoothing features fail to correct for these issues (Fig. 10c). This can result from multiple factors, such as wire leakage (due to failure in the AXBT wire's insulation; Bailey et al. 1994), or a decrease in the signal-to-noise ratio as the aircraft moves farther from the AXBT. Currently there are two manual solutions: 1) adjust the despiking coefficient and smoothing filter length to exclude a greater amount of data points and increase smoothing, or 2) truncate the profile above the depth at which excessive spiking begins to occur. An objective for future work is to implement an autoQC check that automatically performs one of the above corrections when a profile's sliding standard deviation exceeds and remains above a preset threshold.

*(iii) Erroneous mixed layer features*

Accurately quality controlling mixed layer features is both critical and difficult for several reasons. Features such as sea surface and mixed layer temperatures and mixed layer depths are important for air–sea interactions, particularly for observations in tropical cyclones, the purpose for which this program was developed. However, dynamic surface conditions can be difficult to distinguish (qualitatively or programmatically) from probe equilibration with ambient ocean temperature, requiring climatology-informed decisions by the operator. Additionally, boundary conditions can reduce the effectiveness of smoothing filters at removing noise, making it difficult to implement programmatic solutions for erroneous mixed layer features (Fig. 10d). No additional checks have been implemented for mixed layer errors, which require manual quality control after autoQC algorithm application.

*(iv) Spikes due to noise and interference*

Although the autoQC algorithm is designed to identify and correct erroneous spikes from VHF interference, a few profiles had spikes that the algorithm failed to fully remove (Fig. 10e). The autoQC algorithm fails when spikes occur on a length scale greater than the despiking filter window (default 10 m), or when the spike skews the entire distribution of temperature points in a given window so it is no longer centered approximately on the ideally corrected value. No corrections have been implemented to address this shortcoming, which is one reason that manual quality control is still necessary following application of the autoQC algorithm.

*(v) False starts*

The autoQC algorithm was generally extremely effective at identifying and correcting false starts due to VHF interference. In the two profiles where false starts were not detected by the autoQC algorithm, the algorithm failed because either the gap between interference and good data was too small (less than 5 m), or the interference extended without gaps to too great a depth (greater than 50 m; e.g., Fig. 10f). This is because the autoQC false start detection check works by identifying (and

correcting for) lapses in data exceeding a 5 m interval in the upper 50 m of the ocean. These thresholds are sufficient for correcting more subtle interference, whereas interference that the autoQC algorithm fails to detect (e.g., Fig. 10f) is much more obvious and easily detected during manual quality control checks.

## 4. Conclusions

The AXBT Real-Time Editing System (ARES) is a software solution that enables the simultaneous receipt and processing of multiple AXBTs in real time, with a seamless transition to a profile quality control interface. This system integrates generally hardware-defined tasks (signal processing and audio recording) as software-defined functions completed on the processing computer, which minimizes necessary external hardware. ARES can use connected GPS receivers and system date and time to minimize the amount of user inputs (and margin for user error), and supports exporting raw and quality-controlled temperature–depth profiles in several binary and ASCII formats.

The ARES Data Acquisition System provides a high level of user control over the signal processor configuration when receiving data. For tropical Atlantic and Pacific Ocean temperature–depth profiles collected during the TROPIC field program, the signal processing techniques incorporated in ARES reduced spiking due to VHF interference, outperforming the industry standard near the surface and below 200 m. Additionally, this high level of control over signal processing settings enables users to maximize the amount of AXBT signal recovered while optimizing the balance between computational expense and temperature precision for a given processing computer's resources (e.g., random access memory, clock rate) and operational requirements (e.g., AXBT deployment frequency). Finally, the ability to reprocess profiles from digital audio (WAV) files without any external hardware allows users to correct for interference or other discrepancies and to regenerate profiles (when needed) while maintaining a fast work tempo.

The ARES Profile Editor automates the vast majority of necessary profile corrections while providing a simple interface for users to make additional manual edits as necessary. The integrated autoQC algorithm corrects for common modes of VHF interference and integrates bathymetry and climatology to identify and correct additional profile discrepancies. This algorithm had an 87% success rate, correcting all deficiencies for 1021 of 1177 good-quality temperature–depth profiles collected during the TROPIC field program. Additionally, using the ARES Profile Editing System enabled a 9% increase in the number of profiles of sufficient quality for transmission to the GTS while reducing per-profile processing time approximately tenfold.

In conclusion, ARES performed well when evaluated against profiles collected during the TROPIC field program. However, the potential for improved performance remains, and additional, more generalized testing is needed. The autoQC algorithm can be improved to better identify and correct (either by more aggressive spike removal or profile truncation) regions with high signal interference and more efficiently integrate climatology to apply automatic profile corrections. Additionally, the autoQC algorithm should be evaluated against a global dataset of temperature profiles to identify any shortcomings in quality controlling profiles with unique regional characteristics.

*Acknowledgments.* The authors are grateful for the support of the U.S. Air Force Reserve 53rd Weather Reconnaissance Squadron (Hurricane Hunters), who deployed the AXBTs used in this study. Additionally, the authors thank Matthew Kuhn, Jeffrey Kerling, and Kyle Rushing from the Naval Oceanographic Office for their technical guidance, and Jordan Sun, Grace Rovira, Jacob Drogowski, and Shannon McAllister for the numerous hours they spent testing and evaluating the ARES quality control system. This work was sponsored by the Office of Naval Research (Grants N000141812819 and N0001420WX00345) and the U.S. Navy's Civilian Institution Office with the MIT–WHOI Joint Program.

*Data availability statement.* Quality-controlled data collected during the TROPIC field program are available online at https://accession.nodc.noaa.gov/0209221. Individual AXBT profiles, spatial and/or temporal subsets, and additional file types are accessible at http://mmmfire.whoi.edu/tropic/. The AXBT Real-Time Editing System (ARES) source code is available at https://www.github.com/cdens/ares, and supporting data files and an executable installer version of the software are available at http://mmmfire.whoi.edu/ares.

## REFERENCES

Alappattu, D., and Q. Wang, 2015: Correction of depth bias in upper-ocean temperature and salinity profiling measurements from airborne expendable probes. *J. Atmos. Oceanic Technol.*, **32**, 247–255, https://doi.org/10.1175/JTECH-D-14-00114.1.

Amante, C., and B. Eakins, 2004: ETOPO1 1-arcminute global relief model: Procedures, data sources and analysis. NOAA Tech. Memo. NESDIS NGDC-24, 25 pp., https://www.ngdc.noaa.gov/mgg/global/relief/ETOPO1/docs/ETOPO1.pdf.

Bailey, R., A. Gronell, H. Phillips, E. Tanner, and G. Meyers, 1994: Quality control cookbook for XBT data (expendable bathythermograph data) version 1.1. CSIRO Marine Laboratories Rep. 221, 37 pp., http://hdl.handle.net/11329/127.

Bane, J., and M. Sessions, 1984: A field performance test of the Sippican deep aircraft-deployed expendable bathythermograph. *J. Geophys. Res.*, **89**, 3615–3621, https://doi.org/10.1029/JC089iC03p03615.

Boyd, J. D., 1987: Improved depth and temperature conversion equations for Sippican T-5 XBTs. *J. Atmos. Oceanic Technol.*, **4**, 545–551, https://doi.org/10.1175/1520-0426(1987)004<0545:IDATCE>2.0.CO;2.

——, and R. Linzell, 1993: Evaluation of the Sparton tight-tolerance AXBT. *J. Atmos. Oceanic Technol.*, **10**, 892–899, https://doi.org/10.1175/1520-0426(1993)010<0892:EOTSTT>2.0.CO;2.

Cheng, L., and Coauthors, 2016: XBT science: Assessment of instrumental biases and errors. *Bull. Amer. Meteor. Soc.*, **97**, 924–933, https://doi.org/10.1175/BAMS-D-15-00031.1.

Grempler, K., 1993: An improved airborne ocean temperature acquisition display and analysis system. *Johns Hopkins APL Tech. Dig.*, **14**, 253–258.

Hanson, J., 1989: An overview of the System for At-Sea Environmental Analysis (SASEA). *Proc. Oceans*, Seattle, WA, Institute of Electrical and Electronics Engineers, 1658–1664, https://doi.org/10.1109/OCEANS.1989.587139.

Heinmiller, R., C. Ebbesmeyer, B. Taft, D. Olson, and O. Nikitin, 1983: Systematic errors in expendable bathythermograph (XBT) profiles. *Deep-Sea Res.*, **30A**, 1185–1196, https://doi.org/10.1016/0198-0149(83)90096-1.

Kloss, G., 2009: Automatic C library wrapping—Ctypes from the trenches. *Res. Lett. Inf. Math. Sci.*, **13**, 1–7.

Legler, D., and Coauthors, 2015: The current status of the real-time in situ Global Ocean Observing System for operational oceanography. *J. Oper. Oceanogr.*, **8**, s189–s200, https://doi.org/10.1080/1755876X.2015.1049883.

NRL, 2009: Generalized digital environmental model (GDEM). NRL, https://nrlgodae1.nrlmry.navy.mil/ftp/outgoing/static/ocn/gdem/.

Oliphant, T. E., 2006: *A Guide to NumPy*. Vol. 1. Trelgol Publishing, 85 pp.

Roemmich, D., and B. Cornuelle, 1987: Digitization and calibration of the expendable bathythermograph. *Deep-Sea Res.*, **34A**, 299–307, https://doi.org/10.1016/0198-0149(87)90088-4.

Sanabia, E., B. Barrett, P. Black, S. Chen, and J. Cummings, 2013: Real-time upper-ocean temperature observations from aircraft during operational hurricane reconnaissance missions: AXBT demonstration project year one results. *Wea. Forecasting*, **28**, 1404–1422, https://doi.org/10.1175/WAF-D-12-00107.1.

Sessions, M., T. Barnett, and W. Wilson, 1975: The airborne expendable bathythermograph. *Deep-Sea Res. Oceanogr. Abstr.*, **23**, 779–782, https://doi.org/10.1016/S0011-7471(76)80021-6.

Sippican, 2003: Mk-21 ISA bathythermograph data acquisition system installation, operation, and maintenance manual. Sippican Doc., 140 pp., https://pages.uoregon.edu/drt/MGL0910_Science_Report/attachments/MK21_ISA_Manual_Rev_A.pdf.